

Two-color cross-correlation in small-angle static light scattering

Luca Cipelletti,^{*} Marina Carpineti,[†] and Marzio Giglio[‡]

Dipartimento di Fisica and Istituto Nazionale per la Fisica della Materia, Università di Milano, Via Celoria 16, 20133 Milano, Italy

(Received 11 July 1997)

We have measured by means of a charge-coupled device sensor the space correlation function between two speckle fields at different wavelengths. The fields are generated from the scattering of a two-color laser beam from a stationary, three-dimensional sample. In general, the speckle fields attain their maximum degree of correlation when the scattering angles are properly scaled according to a grating dispersion rule. The degree of correlation, however, depends both on the thickness of the sample and on its turbidity. At a given angle, the degree of cross-correlation diminishes as the thickness is increased, and it also decreases as the turbidity grows. Working formulas are derived, and we show that the dependence from the sample turbidity is related to the spread in photon paths. A comparison with the photon path spread calculated by means of a multiple-scattering Monte Carlo simulation will be presented. The connection between the present work and studies on polychromatic light diffraction from random two-dimensional transparencies and microwave transmission through thick samples will also be presented. [S1063-651X(98)15502-2]

PACS number(s): 42.25.Bs, 42.30.Ms, 05.40.+j

I. INTRODUCTION

It is well known that the scattered radiation exhibits *time* fluctuations and shows high contrast intensity *space* variations, as vividly evidenced by the presence of speckles in the scattered pattern [1,2]. At a fixed point, the time correlation function of the intensity scattered by a sample is simply related to the dynamic properties of the scatterers. This is the operating principle of dynamic light scattering, a well established technique that has been successfully used in countless applications. Sophisticated digital correlators are commercially available, and their use is quite widespread to tackle problems in physics, chemistry, biological science, and medicine.

Present day technology makes it possible to record the intensity distribution of a speckle field by means of a charge-coupled device (CCD) sensor. The advantage offered by the CCD over conventional recording techniques is that they provide digitized images of the scattering pattern, which may be directly processed while running the experiment. For processes that are slow enough, a new instrumental procedure for dynamic light scattering measurements has been generated, since parallel correlation function algorithms allow one to determine the time correlation functions as evaluated (in parallel) at various points in the scattered intensity pattern [3]. The use of a CCD sensor is very intriguing and very good quality (equal time) space correlation functions should be obtainable, thanks to the good averaging properties of the process. In view of the fact that time correlation functions give information of great interest, one could ask if the space correlation function would also yield any valuable informa-

tion. The answer is unfortunately negative. Indeed, no information on physical properties of the sample is actually contained in the space correlation function. Statistical optics teaches that the space correlation function is solely related to the actual intensity distribution of the scattering volume, as observed by the region where the speckle pattern is collected [1].

It has been shown, however, that polychromatic speckle techniques can be used to characterize rough surfaces, i.e., two-dimensional (2D) samples. Theory and experiments show that when a rough surface is illuminated by polychromatic light, the speckle pattern exhibits a radial structure revealing a correlation between speckle fields at different wavelengths. Furthermore, a measure of the intensity cross-correlation provides information on the surface roughness [4–7]. In fact, the degree of correlation is related to the statistical properties of the scatterer through the rms value σ_h of its height fluctuation. When σ_h is increased, a gradual decorrelation is observed and ultimately the polychromatic field loses completely its radial structure.

In the present work we study two-color spatial cross-correlation in three-dimensional (3D) static samples. We measure the spatial cross-correlation γ_l varying the sample turbidity τ and we observe that the cross-correlation function is almost insensitive to the increase in turbidity until τ reaches very high values. In fact, at low turbidity the speckle patterns are strongly correlated and, only when the samples become really turbid, the speckle fields finally start to decorrelate. We will show that the loss of chromatic correlation can be interpreted as due to the spread in photon paths in getting out of the sample, caused by the presence of strong multiple scattering. In fact, rampant multiple scattering—inevitably associated with very high turbidities—causes an increase in the width σ_l of the photon path length distribution $p_l(l)$. This spread is responsible for the wave front phase modulation imposed on the beam. We find that, in analogy with the 2D case, substantial decorrelation is attained when the typical depth of the wave front modulation

^{*}Present address: Department of Physics, University of Pennsylvania 209 S 33rd Street, Philadelphia, PA 19104-6396. Electronic address: lucacip@dept.physics.upenn.edu

[†]Electronic address: marina.carpinetti@mi.infn.it

[‡]Electronic address: marzio.giglio@mi.infn.it

is too large, i.e., when $n_s \sigma_l \Delta k \geq 1$, where n_s is the medium index of refraction, $\Delta k = k_1 - k_2$, and $k_{1,2} = 2\pi/\lambda_{1,2}$, $\lambda_{1,2}$ being the vacuum wavelength of the two colors. A test of the above relation has been done by calculating $p_l(l)$ and its standard deviation σ_l via a Monte Carlo simulation of the photon propagation [8]. We find good agreement, although only qualitative, with the proposed model.

The present work is somehow related with two different sets of papers. In the first one [9–12], two wavelength correlation techniques have been used to eliminate from large-angle dynamic light scattering measurements the contributions due to multiple scattering. In spite of the existence of some analogy, this line of research is quite far from that discussed here, as will be clarified in the following. Much stronger connections can be found with the second set of papers [13–16], in which correlation measurements of microwaves in random media are performed as a function of the frequency shifts.

The paper is organized as follows. In Sec. II we describe the experimental setup and the sample. In Sec. III we present both the basic theory and the experimental results for the single scattering regime at low turbidity values. Finally, in Sec. IV we deal with the two-color decorrelation in highly turbid samples and we briefly discuss the connections between the present work and the experiments described in the two sets of papers mentioned above [9–12,13–16].

II. PRINCIPLE OF OPERATION AND EXPERIMENTAL SETUP

Spatial cross-correlation measurements are performed as follows. Two laser beams of different wavelengths are brought to a sample. Each one generates a speckle field. The spatial cross-correlation $\gamma_l(\mathbf{r}_1, \mathbf{r}_2)$ is calculated by multiplying the intensity at one point \mathbf{r}_1 of one speckle pattern by the intensity of the other one at point \mathbf{r}_2 (here and in the following $\mathbf{r}_{1,2}$ describe the points in the far field plane, $r=0$ being the position occupied by the center of the beam when the diffuser is removed). If, as in the present case, the sample is isotropic, the cross-correlation is invariant under rotation around the optical axis. Therefore, the cross-correlation function is obtained by averaging over all points lying on a circle of radius r_1 . We will show that at low angle, the maximum of the cross-correlation function is expected for $k_1 \mathbf{r}_1 = k_2 \mathbf{r}_2$, similarly to the case of 2D samples. This indicates that if the two speckle fields are perfectly correlated, then they can be exactly superimposed by rescaling the lengths according to $\mathbf{r}_2 = (k_1/k_2) \mathbf{r}_1 = (\lambda_2/\lambda_1) \mathbf{r}_1$, where the ratio λ_2/λ_1 between the wavelengths is the dilation factor of the speckle fields.

The experimental setup is sketched in Fig. 1. Two linearly polarized He-Ne laser beams of different wavelengths, namely, $\lambda_1 \equiv \lambda_g = 543.5$ nm (green) and $\lambda_2 \equiv \lambda_r = 632.8$ nm (red), are combined by the beam splitter cube BS, pass through a spatial filter, and impinge onto the sample cell. The setup is arranged so that the size of the beam spot on the cell is the same for the two colors. The cell is mounted on a xy translator whose movement is controlled by a computer guided stepping motor. The optical scheme for the collection of the scattered light is similar to that described by Ferri [17]. Both the scattered and the transmitted light are col-

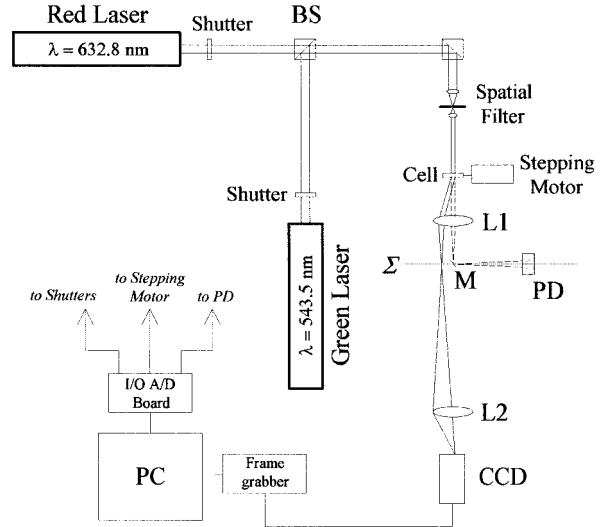


FIG. 1. Schematic diagram of the small-angle static light scattering setup for studying the two-color speckle field cross-correlation.

lected by lens $L1$. In its focal plane Σ , a small mirror M is placed, forming an angle of 45° with the incident beams. The transmitted beams are focused by lens $L1$ onto the mirror and then reflected to photodiode PD. The lens $L2$ is positioned so as to realize a reduced image of the $L1$ focal plane Σ onto the CCD sensor. With this optical scheme, each CCD pixel corresponds to a different scattering wave vector \mathbf{q} , where $q = 4\pi n_s \lambda^{-1} \sin \theta/2$, θ being the scattering angle. Wave vectors of the same magnitude are mapped to pixels lying on a circumference centered around the optical axis position. In the present configuration, the speckle linear dimension is about four CCD pixels and we collect light over a range of angles between 0.4° and 10° . Two shutters, driven by the personal computer (PC), are placed in front of the lasers and allow to select the speckle field of interest. The CCD images are digitized and acquired by the PC via an 8-bit frame grabber.

As the CCD sensor is a black and white one, the speckle patterns of the two colors are separately recorded in sequence, and the two-color spatial intensity cross-correlation function is then calculated. In order to reduce the noise of the cross-correlation function, we average over many pairs of frames (typically 100). Before recording each pair of frames, the cell is moved in the xy plane for obtaining statistically independent speckle patterns, as we used static samples. The calculation of the intensity cross-correlation function γ_l is performed according to the following definition:

$$\gamma_l(\mathbf{q}_1, \mathbf{q}_2) = \gamma_l(q_1, q_2, \Delta\phi) = \frac{\langle I(q_1, \phi_1) I(q_2, \phi_2) \rangle_{q_1}}{\langle I(q_1, \phi_1) \rangle_{q_1} \langle I(q_2, \phi_2) \rangle_{q_2}} - 1. \quad (1)$$

In Eq. (1), $I(q_i, \phi_i)$ is the intensity of the speckle pattern of the i th color at a wave vector magnitude q_i and at an azimuthal scattering angle ϕ_i , $\Delta\phi = \phi_1 - \phi_2$, and $\langle \dots \rangle_{q_i}$ indicates an azimuthal average over pixels with the same wave vector magnitude q_i , i.e., pixels lying on a circumference of radius r_i . Note that the intensity cross-correlation may also

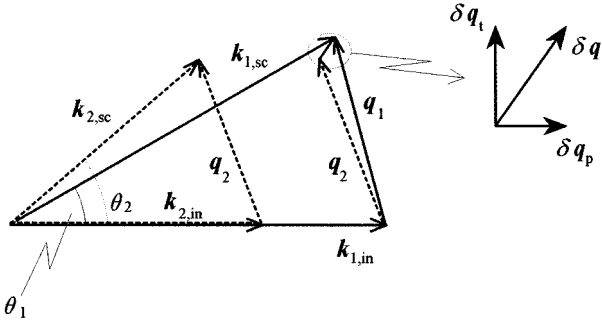


FIG. 2. Scattering vector diagram. The incident \mathbf{k}_{in} , the final \mathbf{k}_{sc} , and the scattering \mathbf{q} wave vectors of the two colors are shown. The difference $\delta\mathbf{q}$ between \mathbf{q}_1 and \mathbf{q}_2 is enlarged to show its transverse $\delta\mathbf{q}_t$ and parallel $\delta\mathbf{q}_p$ components, with respect to the incoming beams direction.

be expressed in a more usual way, as a function of the spatial polar coordinates (in the sensor plane) r_1 , r_2 , $\Delta\phi$: $\gamma_I = \gamma_I(r_1, r_2, \Delta\phi)$. Although, as already pointed out, the statistical properties of the speckle fields are invariant under rotation about the optical axis, they are not invariant under space translation. It follows that γ_I depends on both r_1 and r_2 , while it depends on the azimuthal angles ϕ_1 and ϕ_2 only through the angular lag $\Delta\phi$, as evidenced in writing Eq. (1). In practice, for a given radius r_1 , we restrict the calculation of γ_I to those values of Δr and $\Delta\phi$ for which a significant degree of correlation is expected, i.e., when the green and red \mathbf{q} vectors approximately coincide.

It is to be pointed out that, with the arrangement shown in Fig. 1, it is not possible to collect exactly the same \mathbf{q} vector for the two colors, as the two beams impinge onto the cell along the same direction (see Fig. 2). At low angle, however, the difference $\delta\mathbf{q}$ between the two scattering wave vectors is very small. In particular, $\delta\mathbf{q}$ can be considered negligible if it is less than the uncertainty associated to each \mathbf{q} mode. In fact, there is a natural uncertainty in the measure of \mathbf{q} —due to the finite size of the scattering volume—that is associated with the finite speckles size [18]. It is useful to decompose $\delta\mathbf{q}$ into two components $\delta\mathbf{q}_p$ and $\delta\mathbf{q}_t$ parallel and transverse to the incident beam, respectively (see Fig. 2). We will show in Sec. III that, with the present arrangement, to maximize chromatic correlation the transverse components of the red and green wave vectors must be the same, i.e., $\delta q_t = 0$. Moreover, as will be demonstrated in the following, to observe a significant degree of cross-correlation, δq_p must be less than the typical uncertainty in the parallel component of \mathbf{q} , which is inversely proportional to the sample thickness [18]. As a consequence, in order to have small enough δq_p one needs to work with thin enough samples.

The samples are microporous membrane filters (Sartorius), which have been characterized in a previous work [19], and whose features fit very well the experimental requirements. First of all, the membranes are quite thin, their thickness being $140 \pm 5 \mu\text{m}$. Moreover, while in air they look perfectly opaque, their transmittivity can be increased by permeating them by a properly chosen, quasi-index-matching solvent. Therefore, it is possible to gradually vary the sample turbidity τ by slightly changing the solvent index of refraction. Finally, membranes are static samples, so that the scattered speckle pattern does not change in time. This allows

one to largely simplify the experimental setup, as the two-color speckle fields can be recorded in sequence without any requirement on the CCD and frame grabber speed.

III. CROSS CORRELATION IN THE SINGLE SCATTERING REGIME: THEORY AND EXPERIMENTAL RESULTS

In this section, we focus on the single scattering regime, starting with a brief discussion of the main features of the intensity cross-correlation function. As we anticipated, a significant degree of correlation between the two-color speckle fields is expected when $\delta\mathbf{q} = \mathbf{q}_1 - \mathbf{q}_2 \approx 0$. The dependence of γ_I on $\delta\mathbf{q}$ can be worked out with simple calculations. In analogy to Ref. [11], it can be easily shown that the expression for $\gamma_I(\mathbf{q}_1, \mathbf{q}_2)$ for single scattering alone is

$$\gamma_I(\mathbf{q}_1, \mathbf{q}_2) \approx \left| \frac{\int d^3\mathbf{x} |P(\mathbf{x})|^2 \exp(-i\delta\mathbf{q} \cdot \mathbf{x})}{\int d^3\mathbf{x} |P(\mathbf{x})|^2} \right|^2, \quad (2)$$

where $|P(\mathbf{x})|^2$ is the incident intensity distribution of the scattering volume. If we assume that the sample has thickness d and that the incident beam has a Gaussian profile with radius w at $1/e^2$, then

$$|P(\mathbf{x})|^2 \propto \exp\left(-\frac{2x_r^2}{w}\right) \text{rect}\left(\frac{x_p}{d}\right), \quad (3)$$

where x_r and x_p are the \mathbf{x} components transverse and parallel to the incidence direction and

$$\text{rect } x = \begin{cases} 1, & |x| \leq 1 \\ 0, & |x| > 1. \end{cases}$$

By substituting Eq. (3) in Eq. (2), one obtains

$$\gamma_I(q_1, q_2, \Delta\phi) = \exp\left(-\frac{\delta q_t^2 w^2}{4}\right) \text{sinc}^2 \frac{\delta q_p d}{2}, \quad (4)$$

where $\text{sinc } x = \sin x / x$, and δq_t and δq_p depend on \mathbf{q}_1 and \mathbf{q}_2 only through their magnitudes and their relative azimuthal orientation, due to the rotational symmetry mentioned above.

From Eq. (4) it is now possible to determine under which conditions the maximum intensity cross-correlation may be observed. First of all, from simple geometrical arguments it follows that for a given pair of scattering wave vectors \mathbf{q}_1 and \mathbf{q}_2 , $\delta\mathbf{q}$ is minimum [and therefore γ_I is maximum, see Eq. (4)] when both wave vectors have the same azimuthal direction, i.e., for $\Delta\phi = 0$. Second, for a typical small-angle setup the Gaussian term in Eq. (4) is always narrower than the other one, and it rapidly decays to zero. This is evident in Fig. 3, where the calculated behavior of the two factors in Eq. (4) is sketched as a function of the scattering angle for the red light θ_r , for three different values of θ_g , the green light scattering angle. As a consequence, the Gaussian term fixes the position of the maximum of the cross-correlation function at $\delta q_t = 0$, and its width at $\delta q_t \approx 1/w$, which is the typical uncertainty in \mathbf{q} associated to the speckle size [1,18]. By working out the dependence of δq_t on the scattering angles, it can be easily shown that, at low angle, the conditions $\Delta\phi = 0$ and $\delta q_t = 0$ yield $\tan \theta_r^{\text{max}} = (\lambda_r / \lambda_g) \tan \theta_g$ [see

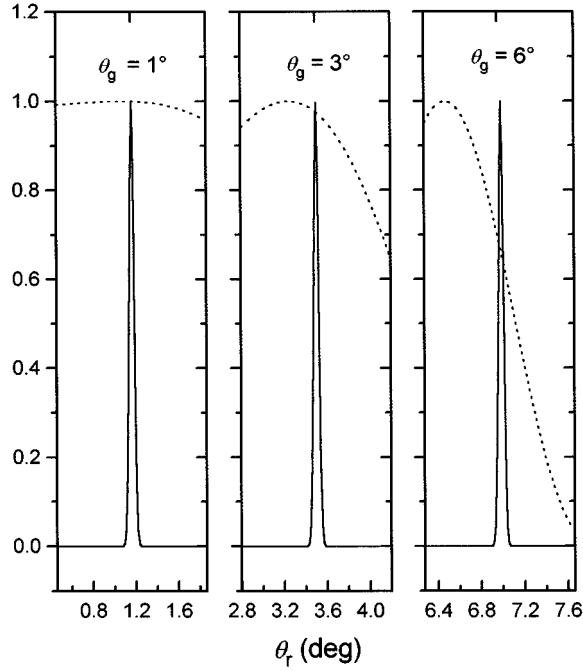


FIG. 3. Calculated behavior of the two factors in Eq. (4) as a function of the red light scattering angle θ_r , for three different values of the green light scattering angle θ_g (see text for more details). The solid line is the $\exp(-\delta q_t^2 w^2/4)$ factor, the dashed line is the $\text{sinc}^2 \delta q_p d/2$ factor. The tick on the upper x axes indicates $\delta q_t = 0$. The intensity cross-correlation γ_I is the product of the two terms plotted above, and is maximum for $\delta q_t = 0$. The two factors were calculated using the same parameters as in the experiment: $\lambda_r = 632.8$ nm, $\lambda_g = 543.5$ nm, $w = 250$ μm , $d = 140$ μm , $n_s = 1.49$.

Appendix A, Eq. (A3)], where θ_r^{max} is the scattering angle of the red light at which the maximum of $\gamma_I(q_1, q_2, \Delta\phi)$ is observed for a given θ_g . Note that, since $r_{r,g} \propto \tan \theta_{r,g}$, the above relation may be written as $r_r = (\lambda_r/\lambda_g)r_g$, as anticipated in Sec. II. This means that, as in the case of rough surfaces, for 3D samples in the single scattering regime the red speckle field is an omothetic version of the green one, the dilation factor being the ratio of the wavelengths λ_r/λ_g . It is to be pointed out that this is the typical scaling law observed when illuminating diffraction gratings with polychromatic light.

We turn now to discuss the second factor in Eq. (4), which has no analog in the case of rough surfaces. We note (see Fig. 3) that the height γ_I^{max} of the peak of cross-correlation is determined by the value of the $\text{sinc}^2 \delta q_p d/2$ factor in correspondence to the maximum of the Gaussian term:

$$\gamma_I^{\text{max}} = \text{sinc}^2 \left(\frac{\delta q_p d}{2} \right) \Big|_{\delta q_t = 0}. \quad (5)$$

As a consequence, it follows that the cross-correlation is gradually lost when increasing the sample thickness d , for a given pair of scattering angles θ_r and θ_g —i.e., for δq_p fixed, see Appendix A, Eq. (A1). Conversely, given d , γ_I^{max} decreases moving towards larger angles, due to the fact that $\delta q_p|_{\delta q_t=0}$ grows with θ_g [see Appendix A, Eq. (A4)]. This sets a limit on the angular range and sample thickness for

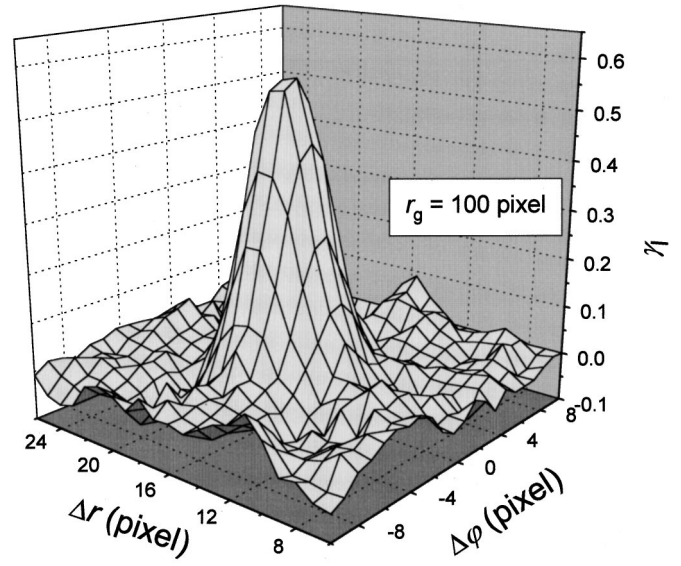


FIG. 4. Intensity cross-correlation γ_I as a function of the radial lag $\Delta r = r_r - r_g$ and of the angular lag $\Delta\phi$, both expressed in pixel. The data were taken at $r_g = 100$ pixels for a low turbidity sample, a Sartorius membrane filter permeated by a quasi-index-matching solvent. The peak at $\Delta r = 16$ pixels and $\Delta\phi = 0$ reveals the radial scaling of the speckle fields when changing the incoming radiation wavelength, according to $r_r/r_g = \lambda_r/\lambda_g \approx 1.16$.

which the two-color intensity cross-correlation may be observed. Moreover, we note from Eq. (5) that, as anticipated, γ_I^{max} is significantly greater than 0 for $\delta q_p \ll 2\pi/d$, i.e., when the magnitude of the parallel component of $\delta\mathbf{q}$ is less than the typical uncertainty π/d of q_p due to the finite thickness d of the scattering volume.

In Fig. 4 a typical example of an intensity cross-correlation function obtained with a sample at low turbidity is shown. The cross-correlation function refers to a green radius $r_g = 100$ pixel (corresponding to a scattering angle θ_g of about 1.4°), and it is plotted as a function of both the radial and the angular lag, expressed in pixel units. The peak of the cross-correlation shown in Fig. 4 reflects the fact that, as discussed above, the red speckle field is the omothetic version of the green one with a dilation factor given by $\lambda_r/\lambda_g \approx 1.16$. In fact, we observe that the maximum correlation is at $\Delta\phi = 0$, and at $\Delta r = 16$ pixel, in good agreement with what was expected as $\Delta r = r_r - r_g = r_g \lambda_r/\lambda_g - r_g$. The width of the peak, that indicates the linear speckle size, is roughly 4 pixels.

In Fig. 5 the behavior of the radial part of the cross-correlation function ($\Delta\phi = 0$) is shown for different values of the green radius r_g (the data shown in Fig. 5 refer to the same sample as in Fig. 4). As already pointed out, the cross-correlation depends both on r_g and on r_r and this is evident by noticing that the peak position moves towards larger r_r as r_g increases. The peak position of the data in Fig. 5 has been compared with the theoretical prediction and the result is shown in Fig. 6, where a plot of $\tan \theta_r^{\text{max}}$ versus $\tan \theta_g$ is presented. Note the remarkably good agreement between the experimental data and the theoretical curve $\tan \theta_r^{\text{max}} = (\lambda_r/\lambda_g) \tan \theta_g$, where no adjustable parameters have been used. With reference to Fig. 5, there is another interesting feature to notice, namely that the peak height decreases as r_g

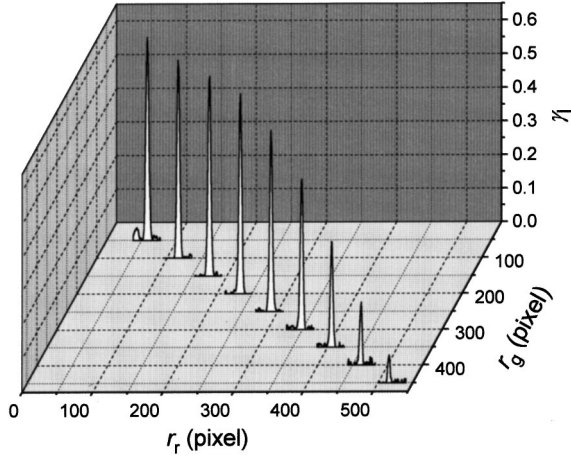


FIG. 5. The radial part of the cross-correlation γ_I as a function of r_r , for various r_g . The sample is the same as in Fig. 4. Note that the peak position shifts towards larger r_r when increasing r_g , according to the radial scaling of the speckle fields of the two colors. At the largest values of r_g , the peak height is reduced due to the thickness of the sample.

increases. This result is a direct consequence of the fact that the difference in \mathbf{q} vectors $\delta\mathbf{q}$ increases as the scattering angle grows, and that ultimately, when matching the transverse component ($\delta q_t = 0$), δq_p becomes even larger than the usual uncertainty in the parallel component of \mathbf{q} .

As a final comment, let us consider the maximum measurable peak height of the cross-correlation function. From the definition of γ_I [see Eq. (1)], it follows that the upper limiting value of λ_I^{\max} is the square of the (monochromatic) speckle field contrast, $C = \sigma_I / \langle I \rangle$, where σ_I is the standard deviation of I . It is well known that the theory predicts $C = 1$ [1]. Actually, from Fig. 4 and from the lower r_g curves in Fig. 5 we observe that $\gamma_I^{\max} \approx 0.6$, which is significantly

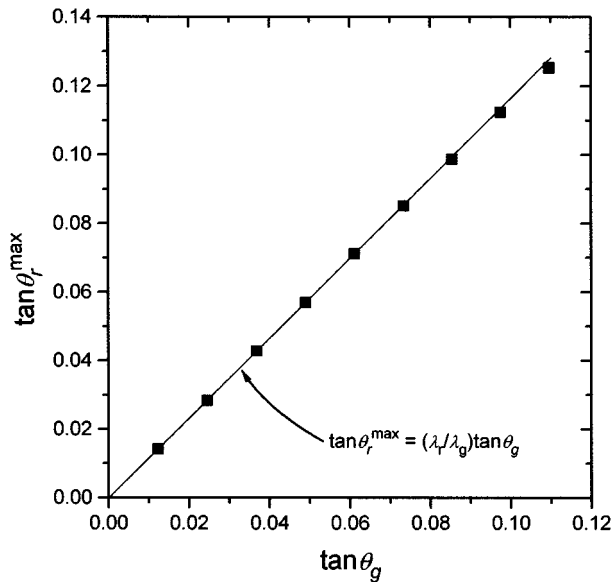


FIG. 6. The peak position of the data shown in Fig. 5. Note the very good agreement between the experimental data (filled squares) and the theoretical line, where not adjustable parameters have been used.

less than 1, although the data were taken at an angle θ_g small enough to prevent any decrease in the peak height due to the sample thickness. This deviation from the theory arises from the data acquisition process. There are two main problems that must be taken into account. The first one is that the CCD pixels have a finite size, while $\gamma_I^{\max} = 1$ is calculated in the hypothesis of pointlike sensors. The effect of the detectors' finite size is just that of reducing both the auto-correlation and the cross-correlation of the speckle fields [1,2]. The second problem is associated with digitalization and saturation effects following from the peculiarities of speckle fields. Speckles appear as very bright spots on a dark background. Consequently, in an experimental recording, the highest intensity value can largely exceed the average value, and it is likely that an appreciable number of pixels reaches the saturation level, even at fairly low average intensity. Therefore, the contrast is underestimated and γ_I^{\max} is lower than expected. One might overcome this problem by reducing the incident beam power. However, at very low average intensity levels, significant distortions in the measured speckle pattern arise from the dark current noise and the digitalization process [20]. We measured the average intensity and the speckle contrast as a function of the incident laser intensity, and the best choice of the latter has been determined on the basis of these tests. We stress that measurements are very reproducible, in spite of the reduced value of γ_I^{\max} with respect to the theoretical value. Therefore, we think that the limitations intrinsic in the use of finite-size detectors and due to digitalization do not severely affect the results.

IV. CHROMATIC DECORRELATION IN HIGHLY TURBID SAMPLES: EXPERIMENTAL RESULTS AND DISCUSSION

We have performed measurements of the cross-correlation function for different sample turbidities. As already explained, it is possible to vary the turbidity by using solvents with different index of refraction n_s . We used acetate of cellulose membranes (Sartorius SM 123 03) with an index of refraction $n \approx 1.47$ permeated by solvents of increasing n_s , with $n_s > n$. In Fig. 7 a plot of the maximum of the intensity cross-correlation γ_I^{\max} as a function of n_s , is shown. All the measurements of γ_I^{\max} have been performed at the same scattering angle $\theta_g \approx 0.7^\circ$ ($r_g = 50$ pixels), corresponding to $q_g = 2100 \text{ cm}^{-1}$, which is small enough to prevent a significant decorrelation due to sample thickness. From Fig. 7 it is evident that the cross-correlation peak value decreases as the optical mismatch—and therefore the turbidity—increases.

In order to explain the observed loss of cross-correlation, it is useful to reconsider the basic results of the works performed on 2D samples [4–7]. Two-color speckle fields generated by rough surfaces are highly correlated when $\Delta k(n-1)\sigma_h < 1$, where n is the refractive index of the diffuser and σ_h is the rms value of its height fluctuations. When the surface roughness is increased, the fields start to significantly decorrelate. In particular, it can be shown [4,5] that the intensity cross-correlation function is given by

$$\gamma_I(\mathbf{q}_1, \mathbf{q}_2) = |\Phi_h(\delta q_p)|^2 |\mu(\delta \mathbf{q}_t)|^2, \quad (6a)$$

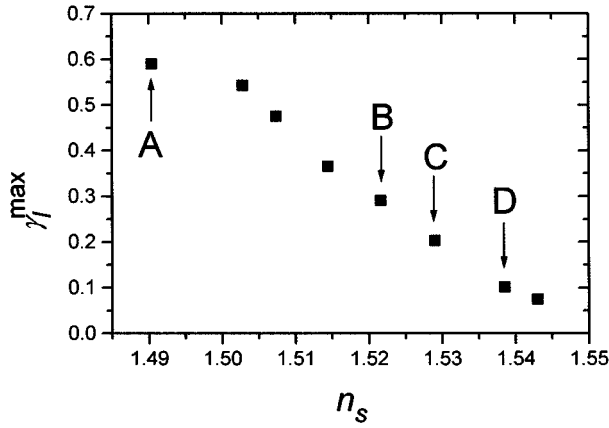


FIG. 7. The intensity cross-correlation peak height γ_I^{\max} as a function of the refractive index of the solvent. The refractive index of the sample is $n \approx 1.47$. The cross-correlation is gradually lost when increasing the refractive index mismatching, and therefore the sample turbidity. The letters in the figure are for future reference.

where $\mu(\delta\mathbf{q}_t)$ is the so-called complex coherence factor, and $\Phi_h(\delta q_p)$ is the characteristic function of the height probability density $p_h(h)$ [1]:

$$\mu(\delta\mathbf{q}_t) = \frac{\int d^3\mathbf{x} |P(\mathbf{x})|^2 \exp(i\mathbf{x} \cdot \delta\mathbf{q}_t)}{\int d^3\mathbf{x} |P(\mathbf{x})|^2}, \quad (6b)$$

$$\Phi_h(\delta q_p) = \int dh p_h(h) \exp(ih \delta q_p).$$

[Incidentally, we note that for a Gaussian incident beam, the $|\mu(\delta\mathbf{q}_t)|^2$ term in Eqs. (6a) and (6b) is exactly the same as the Gaussian factor in Eq. (4).] From Eqs. (6a) and (6b), it follows that γ_I depends on the diffuser only through the characteristic function $\Phi_h(\delta q_p)$. In the hypothesis of a Gaussian distribution of the diffuser height, it can be shown that at small angles Φ_h does not depend on δq_p [20]:

$$\Phi_h = \exp[-\Delta k^2 (n-1)^2 \sigma_h^2], \quad (7)$$

Since Φ_h is independent from \mathbf{q}_1 and \mathbf{q}_2 , it can be easily understood that for 2D samples $\mu(\delta\mathbf{q}_t)$ fixes the peak position of $\gamma_I(\mathbf{q}_1, \mathbf{q}_2)$ at $\delta q_t = 0$, while the second factor in Eq. (6a), Φ_h , is responsible of its height. The validity of Eqs. (6a) and (7) has been verified both qualitatively [4,6] and quantitatively [7] in the past.

It is to be noted that it is impossible to distinguish whether the wave front deformations of the scattered field immediately after the cell have been introduced by a 2D or by a 3D sample. What is actually different is the physical mechanism that generates the phase variations, although in both cases they depend on the differences in photon optical path lengths for crossing the sample. For 3D samples, the different path length of the photons is determined by the amount of multiple scattering. In fact, photons that undergo a few scattering events travel a shorter path when compared to those scattered many times. Moreover, we point out that, as the turbidity grows, multiple scattering of higher orders be-

comes more likely, and so do long photon paths, thus increasing the spread in path lengths. The analogy with the case of rough surfaces suggests that the chromatic decorrelation is determined by the spread in path lengths. To be more explicit, the analogous of $(n-1)\sigma_h$ for 3D samples is the spread $n_s\sigma_l$ of the photon optical path length distribution inside the sample, σ_l being the standard deviation of the geometrical photon path distribution $p_l(l)$. Consequently, we expect that the fields will start to significantly decorrelate when

$$\Delta k n_s \sigma_l \geq 1. \quad (8)$$

A similar result was obtained in the past in works on microwave propagation in random media [13–16]. The authors performed cross-correlation measurements varying the wave frequency and they relate the decorrelation to the spread in photon travel times through the sample. Furthermore, they show that the intensity-intensity correlation as a function of frequency shift is the squared modulus of the Fourier transform of the photon time-of-flight distribution [15]. We recall that Eqs. (6a) and (6b) link the two-color intensity cross-correlation to the Fourier transform of the photon optical path distribution. Therefore, there is a strong analogy between the results reported in Ref. [15] in the time domain for microwave propagation, and those described in the space domain for light scattered by 2D samples. It is quite remarkable that the two descriptions that apply to quite different electromagnetic spectral regions have the same physical root.

We will now compare the loss of cross-correlation with the spread of the photon path length distribution, calculated by means of a Monte Carlo simulation of the photon propagation. The Monte Carlo multiple-scattering code is described in detail in Ref. [8]. We simply recall here that the simulation consists in tracking the path of a great number of photons through the sample. For each launched photon, track is kept of the length of the path in getting out of the sample, so that the photon path length distribution $p_l(l)$ can be calculated for all q vectors of interest. The main required input parameters are the single scattering differential cross section and the turbidity τ of the sample or, equivalently, its transmission T . The differential scattering cross section was that obtained, for the same sample, in Ref. [8]. The measurement of the sample transmission deserves a brief comment. At low turbidity, T can be directly measured thanks to the photodiode PD (see Fig. 1), by dividing the transmitted beam power in the presence of the sample by that with the cell filled with the solvent alone. For highly turbid samples, however, the transmitted power can be comparable to, or even lower than, the power of the light scattered at extremely low angle, collected together with the transmitted beam by the tiny mirror M , due to its finite size. Therefore, there is a comparatively high spurious signal on PD that leads to a significant overestimation of T . The correct value of the transmission can be recovered by iteratively running the simulation program. One starts with a guess for T to obtain the simulated total light collected by M (scattered light plus transmitted beam). The initial estimate is then refined by comparing the result of the simulation with the experimental data, and a corrected value of T is input for a second run. The entire process is repeated until the simulated power converges to the measured one. Thanks to this procedure, it has been possible to estimate the transmission even for the more turbid samples,

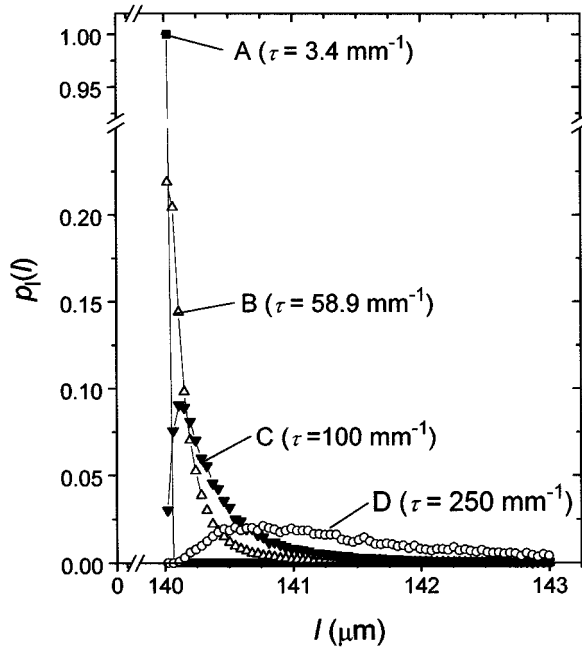


FIG. 8. Photon path length distribution $p_l(l)$, calculated via the Monte Carlo simulation described in the text, for different values of the sample turbidity τ . The curves are labeled with the same letters as the points in Fig. 7.

for which a direct measurement of T would not have been feasible. As a check for the correction procedure, we have also estimated τ for the most turbid samples by extrapolating the low refractive index dependence of the turbidity versus n_s . The corrected data are in reasonable agreement with the extrapolated ones, the maximum deviation being less than 30%.

We have calculated the photon path length distributions $p_l(l)$ and their standard deviation value σ_l for each experimental point shown in Fig. 7 but the last one, for which T was too high to be estimated in a sensible way, even via the Monte Carlo simulation. Figure 8 shows some examples of the calculated $p_l(l)$, for different values of the turbidity. Filled squares refer to the case $\tau = 3.4 \text{ mm}^{-1}$, corresponding to $T = 62\%$, for which the maximum cross-correlation peak value has been measured. As can be seen, $p_l(l)$ vanishes for $l > 140 \text{ } \mu\text{m}$ —i.e., for photon paths longer than the sample thickness—in agreement to what is expected due to the fact that single scattering prevails (see Table I). As the turbidity increases, multiple scattering becomes appreciable and this leads to a larger standard deviation σ_l of $p_l(l)$ (see curves B, C, and D in Fig. 8). As discussed above, we expect that the increase in the photon path length spread is responsible of the cross-correlation loss and that the speckle fields of the two colors significantly decorrelate for $\Delta kn_s \sigma_l \geq 1$. In order to verify this statement, we have plotted in Fig. 9 the experimentally measured maximum value of the cross-correlation function γ_I^{max} as a function of $\Delta kn_s \sigma_l$. Note that the behavior of γ_I^{max} is in good agreement with the one qualitatively expected, as it is significantly reduced when $\Delta kn_s \sigma_l \geq 1$.

As a final point, let us consider the analogies between the present experiment and a two-wavelength cross-correlation technique, proposed in the past for large-angle dynamic light scattering measurements of very turbid samples [9–12]. In

TABLE I. We report, for various values of the solvent refractive index n_s , the measured cross-correlation peak height γ_I^{max} and the ratio between the single and total scattering intensity, I_s/I_t , calculated via the Monte Carlo simulation. In the last column, we show the ratio $\gamma_I^{\text{max}}/(I_s/I_t)^2$, which would be constant if multiple scattering contributions were uncorrelated. The enormous increase in $\gamma_I^{\text{max}}/(I_s/I_t)^2$ clearly indicates that in the present case also multiply scattered photons contribute to the cross-correlation.

n_s	γ_I^{max}	I_s/I_t	$\gamma_I^{\text{max}}/(I_s/I_t)^2$
1.4904	0.59	0.92	0.70
1.5028	0.54	0.61	1.45
1.5074	0.48	0.41	2.86
1.5144	0.37	0.18	11.4
1.5216	0.29	0.03	322
1.5290	0.20	0.02	500
1.5385	0.10	$< 1 \times 10^{-4}$	$> 10^7$

that case, the technique allows one to suppress multiple scattering contributions by cross-correlating the scattered light of two wavelengths, collected at different angles chosen so that the single scattering wave vectors exactly coincide. It can be shown that the time dependence of the cross-correlation function is solely due to single scattering. The two techniques, however, are substantially different. In particular, we stress that in the present experiment the loss of cross-correlation when the sample turbidity increases cannot be explained by assuming that the multiply scattered contributions are uncorrelated. It can be shown (see Appendix B) that, if the singly scattered contributions were the only correlated ones, then γ_I^{max} would be proportional to $(I_s/I_t)^2$, where I_s and I_t are the single and the total scattered intensity, respectively. The ratio I_s/I_t for the data shown in Fig. 7 has been calculated by means of the simulation program de-

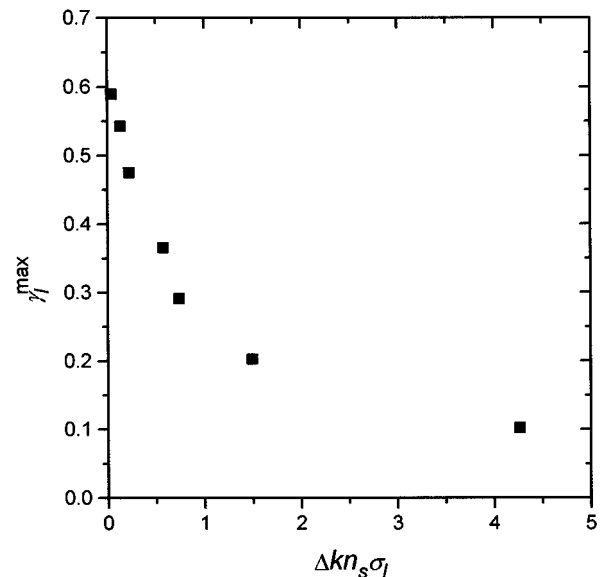


FIG. 9. The measured intensity cross-correlation peak height γ_I^{max} as a function of $\Delta kn_s \sigma_l$, where σ_l has been calculated via the Monte Carlo photon propagation simulation. The cross-correlation between the two-color speckle fields is substantially lost when $\Delta kn_s \sigma_l \geq 1$.

scribed above and is reported in Table I, together with $\gamma_I^{\max}/(I_s/I_t)^2$. It can be noted that the ratio $\gamma_I^{\max}/(I_s/I_t)^2$ enormously increases with the amount of multiple scattering, thus demonstrating that single scattering contributions are not the only correlated ones.

The main differences between the two techniques are the following. First, we do not collect light so that the scattering q vector is exactly the same for the two wavelengths, as in the two-color dynamic light scattering apparatus. Second, we collect light at small angles and use samples with a differential scattering cross section strongly peaked near the forward direction [19], while in a typical two-color dynamic light scattering setup measurements are performed at much larger angles [12], and using small scatterers, which diffuse light almost isotropically. As a consequence, for the dynamic light scattering experiment the two-color wave vectors associated to each intermediate scattering event are generally much different, and the only significantly correlated are the singly scattered ones. Conversely, in the present experiment the differences between the intermediate scattering vectors for the two colors are so small that they turn out to be comparable to the unavoidable difference $\delta\mathbf{q}$ between the final wave vectors. Therefore, even light scattered more than once probes essentially the same fluctuation Fourier modes for the two colors. Note that the same reason for which we are able to observe correlation with the present configuration—i.e., that $\delta\mathbf{q}$ is smaller than the natural uncertainty in \mathbf{q} —is responsible for the correlation between multiply scattered contributions. Only when a large number of scattering events occurs, the small differences in the intermediate wave vectors may sum up and finally overcome $\delta\mathbf{q}$, giving rise to a significant loss of cross-correlation.

To summarize, we have performed measurements of two-wavelength spatial cross-correlation between the intensities

scattered at small angles by thin 3D samples. We have used an experimental setup that allows to record the intensity distribution of the speckle fields, thanks to a CCD sensor. We have shown that, in order to observe a significant degree of cross-correlation, it is necessary for the difference between the scattering wave vectors to be small compared with the natural uncertainty in \mathbf{q} associated with the finite sample thickness. Furthermore, we have observed that cross-correlation is gradually lost when the sample turbidity is increased. We have suggested that this effect is associated with the spread in photon path lengths caused by multiple scattering. We have tested this guess thanks to a Monte Carlo simulation of photon propagation, and a qualitative good agreement between the model and the experimental data has been found.

ACKNOWLEDGMENTS

The authors thank D. A. Weitz for useful discussions and for bringing to their attention the papers by A. Z. Genack *et al.* They also wish to thank F. Ferri for suggestions in designing parts of the instrument. This work was partially supported by the Ministero dell'Università e della Ricerca Scientifica e Tecnologica (MURST) and by the Agenzia Spaziale Italiana (ASI).

APPENDIX A

In this appendix we work out the dependence of δq_p and δq_t on the wave vectors k_1 and k_2 of the two-color incident light, and on the scattering angles θ_1 and θ_2 for the two colors. We will refer to the case $\Delta\phi=0$ shown in Fig. 2. From simple geometrical calculations, one gets

$$\delta q_p = n_s \frac{k_1 \sqrt{1 + \tan^2 \theta_2} - [k_2 + (k_1 - k_2) \sqrt{1 + \tan^2 \theta_2}] \sqrt{1 + \tan^2 \theta_1}}{\sqrt{1 + \tan^2 \theta_1} \sqrt{1 + \tan^2 \theta_2}}, \quad (\text{A1})$$

$$\delta q_t = n_s \frac{k_1 \tan \theta_1 \sqrt{1 + \tan^2 \theta_2} - k_2 \tan \theta_2 \sqrt{1 + \tan^2 \theta_1}}{\sqrt{1 + \tan^2 \theta_1} \sqrt{1 + \tan^2 \theta_2}}. \quad (\text{A2})$$

As discussed in Sec. III, maximum cross-correlation is observed for $\delta q_t=0$. Accordingly, to find the relation between θ_1 and θ_2 at the γ_I peak position, we set the numerator of Eq. (A2) to zero, we expand in Taylor series in $\tan\theta_1$ and $\tan\theta_2$ up to the first order, and we solve for $\tan\theta_1$:

$$\tan\theta_2|_{\delta q_t=0} \equiv \tan\theta_2^{\max} = \frac{k_1}{k_2} \tan\theta_1 = \frac{\lambda_2}{\lambda_1} \tan\theta_1. \quad (\text{A3})$$

Finally, we calculate the δq_p value at the cross-correlation peak position. Substitution of Eq. (A3) into Eq. (A1) yields, up to the second order in $\tan\theta_1$,

$$\delta q_p|_{\delta q_t=0} = \frac{1}{2} \frac{k_2}{k_1} n_s (k_1 - k_2) \tan^2 \theta_1. \quad (\text{A4})$$

APPENDIX B

In this appendix we will show that, if multiple scattering contributions to the two-color scattered field were uncorrelated, then γ_I^{\max} would be proportional to $(I_s/I_t)^2$, where I_s and I_t are the single and the total (single plus multiple) scattered intensity, respectively.

We start by recalling that the Siegert relation [10] allows us to express $\gamma_I(\mathbf{q}_1, \mathbf{q}_2)$ through the field cross-correlation $\gamma_A(\mathbf{q}_1, \mathbf{q}_2)$:

$$\gamma_I(\mathbf{q}_1, \mathbf{q}_2) = |\gamma_A(\mathbf{q}_1, \mathbf{q}_2)|^2, \quad (\text{B1})$$

where

$$\gamma_A(\mathbf{q}, \mathbf{q}_2) = \frac{\langle A(\mathbf{q}_1)A^*(\mathbf{q}_2) \rangle}{\sqrt{I(q_1)I(q_2)}}, \quad (\text{B2})$$

and $A(\mathbf{q})$ is the scattered field. If we assume, as in Ref. [11], that only single scattering contributes to γ_A , then in the presence of multiple scattering

$$\langle A_t(\mathbf{q}_1)A_t^*(\mathbf{q}_2) \rangle = \langle A_s(\mathbf{q}_1)A_s^*(\mathbf{q}_2) \rangle = \gamma_{A,s} \sqrt{I_s(\mathbf{q}_1)I_s(\mathbf{q}_2)}. \quad (\text{B3})$$

In Eq. (B3) subscripts s and t refer as usual to single and total scattering, respectively, and $\gamma_{A,s}$ is the field cross-correlation that would have been observed if single scattering alone were present [see Eq. (B2)]. Equations (B1), (B2), and (B3) yield

$$\gamma_I(\mathbf{q}, \mathbf{q}_2) = |\gamma_{A,s}(\mathbf{q}_1, \mathbf{q}_2)|^2 \frac{I_s(q_1)I_s(q_2)}{I_t(q_1)I_t(q_2)}. \quad (\text{B4})$$

Since the maximum intensity cross-correlation is observed for $q_1 \approx q_2 \equiv q$, from Eq. (B4) we obtain

$$\gamma_I^{\max}(q) = |\gamma_{A,s}(q)|^2 \left(\frac{I_s(q)}{I_t(q)} \right)^2. \quad (\text{B5})$$

For a given sample thickness and a given scattering wave vector q , $\gamma_{A,s}$ is a constant and does not depend on the amount of multiple scattering. Therefore, Eq. (B5) shows that the cross-correlation peak height is proportional to the square of the fraction of single scattering intensity.

-
- [1] J. W. Goodman, in *Laser Speckle and Related Phenomena*, edited by J. C. Dainty (Springer-Verlag, Berlin, 1975); J. W. Goodman, *Statistical Optics* (Wiley, New York, 1985).
- [2] See, for example, B. J. Berne and R. Pecora, *Dynamic Light Scattering* (Wiley, New York, 1976).
- [3] A. P. Y. Wong and P. Wiltzius, *Rev. Sci. Instrum.* **64**, 2547 (1993).
- [4] G. Parry, *Opt. Commun.* **12**, 75 (1974).
- [5] G. Parry, in *Laser Speckle and Related Phenomena* (Ref. [1]).
- [6] G. Tribillon, *Opt. Commun.* **11**, 172 (1974).
- [7] M. Giglio, S. Musazzi, and U. Perini, *Opt. Commun.* **28**, 166 (1978).
- [8] L. Cipelletti, *Phys. Rev. E* **55**, 7733 (1997).
- [9] G. D. J. Phillies, *J. Chem. Phys.* **74**, 260 (1981).
- [10] J. K. G. Dhont and C. G. De Kruif, *J. Chem. Phys.* **79**, 1658 (1983).
- [11] K. Schätzel, *J. Mod. Opt.* **38**, 1849 (1991).
- [12] P. N. Segrè, W. Van Megen, P. N. Pusey, K. Schätzel, and W. Peters, *J. Mod. Opt.* **42**, 1929 (1995).
- [13] A. Z. Genack, *Phys. Rev. Lett.* **58**, 2043 (1987).
- [14] N. Garcia and A. Z. Genack, *Phys. Rev. Lett.* **63**, 1678 (1989).
- [15] A. Z. Genack and M. Drake, *Europhys. Lett.* **11**, 331 (1990).
- [16] A. Z. Genack, N. Garcia, and W. Polkosnik, *Phys. Rev. Lett.* **65**, 2129 (1990).
- [17] F. Ferri, *Rev. Sci. Instrum.* **68**, 2265 (1997).
- [18] See, for example, G. B. Benedek, in *Statistical Physics, Phase Transition and Superfluidity*, edited by M. Chretien, E. P. Gros, and S. Deser (Brandeis University, Waltham, MA, 1966), Vol. 2.
- [19] L. Cipelletti, M. Carpineti, and M. Giglio, *Langmuir* **12**, 6446 (1996).
- [20] L. Cipelletti, Ph.D. thesis, University of Milan, Italy, 1997.